Relationship between Phenolic Adhesive Chemistry and Adhesive Joint Performance: Effect of Filler Type on Fraction Energy*

ROBERT O. EBEWELE,† *Department of Chemical Engineering, Ahmadu Bello University, Samaru-Zaria, Nigeria,* BRYAN H. RIVER, *Forest Products Technologist, Improved Adhesives Systems, U.S. Forest Products Laboratory, P.O. Box 5130, Madison, Wisconsin 53705,* and JAMES A. KOUTSKY, *Department of Chemical Engineering, University of Wisonsin, Madison, Wisconsin 53706*

Synopsis

The performance of adhesive bonded joints depends on many factors, one of which is the adhesive formulation. The effects of organic and inorganic fillers upon the fracture toughness of phenol–resorcinol–formaldehyde adhesive in hard maple joints were explored in this study. Analytical techniques (DSC, IR, SEM, and GPC), and solubility studies were employed to relate physical effects to chemical effects of the fillers. The resin showed two distinct stages of cure: (1) a low temperature exotherm associated with resorcinol and paraformaldehyde and (2) a high temperature endotherm associated with the base resin. Filler was found not to affect the cure. Fillers did have a profound effect on the morphology of the wood-adhesive interphase and upon the bulk adhesive properties. These effects, revealed in both SEM and fracture toughness studies, are discussed at length.

INTRODUCTION

The long-term stability or durability of adhesive joints has been of primary concern for many years. The service life of an adhesive-bonded structure is determined by its response to a host of successively imposed interrelated conditions. These start from the joint-forming variables and continue through the myriad number of environmental conditions encountered during the course of its structural existence. The performance of an adhesive joint and hence the suitability of an adhesive for a specific application is almost always judged by the strength of the joint (of course, high strength is a necessary but certainly not a sufficient condition for durability). When an adhesive-bonded assembly is loaded to failure, the locus of failure may be in the adherend, in the adhesive, at the adherend–adhesive interface, or any combination of these locations, where failure originates depends upon the magnitude and direction of the imposed stresses in relation to the zone weakness. Values obtained from strength tests, therefore, reflect the inherent variability in the mechanical properties of the individual elements of the bonded assembly. Thus a logical starting point

* Work done at the Uniersity of Wisconsin, Madison.

† To whom inquiries should be addressed.

Journal of Applied Polymer Science, Vol. 31, 2275–2302 (1986)
 CCC 0021-8995/86/072275-28$04.00

in understanding joint performance, vis-à-vis durability, is a fundamental understanding of the properties of these elements. This calls for proper characterization of adhesive and the adherends.

Wood is the adherend used in this study. It is a complex composite engineering material. Its surface chemistry, which plays a vital role in bond formation, is little understood. Its physical condition can significantly affect not only its interaction with the adhesive but can also determine the actual stress distribution in the joint under applied loads. We have previously reported the effects of surface roughness and the nature of surface roughness on joint strength.[1]

Like adherends, the intrinsic properties of the adhesive significantly influence joint performance. Phenol–resorcinol–formaldehyde (PRF) is the base resin in the adhesive used for these studies. Generally, a thermosetting resin adhesive is composed of (1) the base resin, (2) hardener, and (3) filler. The variation of each, or a combination of these components, affects adhesive joint performance. In this article, attention is focused on the effect of filler type on adhesive joint performance. The analytical tools employed in this study include differential scanning calorimetry (DSC), infrared spectroscopy (IR), gel permeation chromatography (GPC), and solubility measurements.

ADHESIVE JOINT STRENGTH MEASUREMENT—THE FRACTURE MECHANICS APPROACH

Fracture mechanics is a relatively new discipline which relates the fracturing behavior of flawed bodies to applied loads. Fracture mechanics is a direct outgrowth of the Griffith theory which postulates that the lower-than-ideal fracture strength of all real bodies is due to the presence of initial flaws or cracks. These may be dust particles, bubbles or nonbonded areas, in the case of adhesive joints. Failure usually occurs by a propagation of the largest of these cracks. Using the concepts of fracture mechanics, one defines fracture toughness which determines the load-bearing capacity of a structure in the presence of flaws.

The stress field in the vicinity of a crack tip can be adequately defined by the parameter K, the stress intensity factor. This parameter, a function of applied load and crack size, increases to a critical value $K = K_c$, whereupon a previously stationary or slow-moving crack propagates abruptly. This critical value, K_c, defines the fracture toughness. For adhesive joints, the analysis required to describe the stress field at the crack tip is extremely difficult. Consequently, fracture toughness is defined in terms of energy by exploiting the relationships between K and the strain-energy release rate G. G is related to K by the equations:

$$\begin{aligned} G &= K^2/E(1 - \nu^2) \quad &&\text{for plane strain} \\ G &= K^2/E \quad &&\text{for plane stress} \end{aligned} \tag{1}$$

where E = Young's modulus, ν = Poisson's ratio, and G = a physical measure of the rate of release of strain energy at the crack tip. For mode I or opening mode, which is the mode of failure of the vast majority of

engineering materials, a cleavage stress field surrounds the crack tip. In this case $K_c = K_{I_c}$ and hence $G_c = G_{I_c}$. Mostovoy et al.[2,3] and Ripling et al.[4-6] have developed and applied the tapered double cantilever beam (TDCB) geometry to a number of composite systems using metal adherends. We have adapted this for use in wood-based adhesive systems. Details of this have been given elsewhere.[1,7] Using the TDCB, the fracture energy is given by the equation

$$G_{I_c} = \frac{4P_c^2}{Eb^2} m \tag{2}$$

where P_c = critical load necessary to cause a previously stationary or slow-moving crack to propagte abruptly, b = width of beam, m = a constant chosen so that compliance changes linearly with crack length, $m = 0.52$ cm^{-1} (1.33 $in.^{-1}$) for all specimens in this study, and E = bending modulus of adherends. At P_c, the crack propagates until enough energy is released to bring the crack to rest. The arrest load value, given by P_a, is related to fracture energy by the equation

$$G_{I_a} = \frac{4P_a^2}{Eb^2} m \tag{3}$$

The condition of stable crack growth is defined when $P_c = P_a (G_{I_c} = G_{I_a})$. The load-deflection profile is a continuous horizontal line in this situation. This is often the case with viscoelastic and ductile materials and very weak interfaces. This contrasts with brittle systems where distinct initiation and arrest load values ($P_c \neq P_a$) result in a saw-tooth load–deflection profile.

EXPERIMENTAL

Materials

Adhesive

The resin used was Koppers Penacolite G4411, a two-part phenol–resorcinol resin, dissolved in a solvent (generally an alcohol). Two lignocellulosic and four inorganic fillers were chosen based on a classification proposed by Robertson and Robertson.[8] The fillers and their pertinent properties are listed in Table I. The hardener used was paraformaldehyde obtained from the Celanese Co.

Adherend

Hard maple (Acer saccharum Marsh) was chosen as the wood substrate because of its high modulus and controllable adhesive assimilation. Rough lumber for the specimens was conditioned to equilibrium at 23°C and 44% RH ($\cong$ 8% EMC). After conditioning, the specimens were cut in such a way as to maintain a specified grain angle to the bonding surface, and then contoured to the appropriate shape. The fracture mechanics approach for evaluation of adhesive strength was followed in these tests.

TABLE I
Adhesive Fillers Used

Filler (supplier)	Chemical composition	pH[a]	Particle size[b]		Shape[b]
			Median diameter (μm)	Screen analysis	
A. Lignocellulosic (organic)					
Walnut shell flour	NA[c]	4.5	NA	NA	Fiber
Bohemia Douglas fir bark extender 100 (Bohemia Inc.)	Douglas fir bark, solvent extracted and sized	3.7	NA	+100 mesh=5%	Granualar and fibrous
B. Inorganic					
Mica (Marietta Res. Int.)	Highly delaminated and pure phlogopite mica flake	NA	—	>325 92%	Flake
Volclay Hi Gel (American Colloid)	Bentonite Clay hydrous aluminum silicate	8.6	NA	+200 mesh <20%	Plate
Celaton MN-41 (Eagle Picher)	Diatomaceous Silica	6.5	3.5	+325 mesh = 5%	NA
Amorphous Silica 200 (Illinois Minerals)	Silica	7	NA	200 mesh 90/95	NA

[a] Equilibrium pH obtained from water dispersions of filler.
[b] Information from supplier.
[c] NA = not available.

Differential Scanning Calorimetry (DSC)

The DSC was employed for screening adhesive formulation variables and deriving preliminary bonding process conditions. Five grams of the resin and the appropriate amount and type of filler and the curing agent were mixed thoroughly in a beaker for 5 min. From this, between 5 and 10 mg was weighed very accurately into a DuPont aluminium-coated pan and then sealed hermetically. Thermograms were then obtained on a DuPont 900 DSC unit using a similarly sealed empty pan as the reference. A heating rate of 10°C/min and a range setting of 4 mcal/s were employed. The temperature range of the scans was 20–300°C. The instrument was calibrated by measuring the heat of fusion of indium. Areas under the peaks were measured with a plannimeter with measurement errors of less than 10%.

Bonding

The adhesive formulation was 100 g resin to 10 g filler to 10 g paraformaldehyde. The adhesive was mixed vigorously by hand for 10 min and then hand-brushed as uniformly as possible on both surfaces of the beams to be mated. Open assembly time was less than 30 s. A small Mylar or Teflon film of 2.54×10^{-3} cm (1 mil) thickness was inserted at the jaw of the specimen to provide the initial flaw. The specimens were placed in a press capable of holding two specimens as shown in Figure 1. The closed assembly time was 30 min. Glueline pressure [1.03–1.17 MPa (150–170 psi)] was measured by a precalibrated compressometer. Before curing, excess adhesive was cleaned off the joint with a knife. The press with the samples was placed in a forced-air oven maintained at 85°C (±1°C) and cured for 1 h. Generally the applied glueline pressure dropped considerably by the time the specimens were removed from the oven due to the combined effects of wood and adhesive drying and metal expansion.

Fracture Testing

After bonding, specimens were conditioned to equilibrium (≅ EMC 8%) at 23°C and 44% RH before fracture tests. A Riehle (Ametek) Universal Testing Machine was employed for these tests as shown in Figure 2. The progress of the crack was monitored by shining a bright light on the rear of the specimen and marking the most extreme location of the emergent light after crack arrest. During testing, all the lights in the room (except the one at the rear of the specimen) were turned off. Sample deflections were measured by an LVDT (Daytronic Signal Conditioner Model 300D). Load and strain values were recorded on a Hewlett Packard HP-70004B X-Y recorder. A crosshead speed of 0.2 mm/min was used. No effect of crosshead speed on G_{I_c} was noted at this or slower speeds. The data approximated dead load conditions where strain rates are very small.

Initial Resin Viscosity

The commercial resin, Penacolite G4411, is usually supplied in an alcohol solution. Preliminary experiments and the literature had indicated that initial resin viscosity has some effect on fracture energy. This was inves-

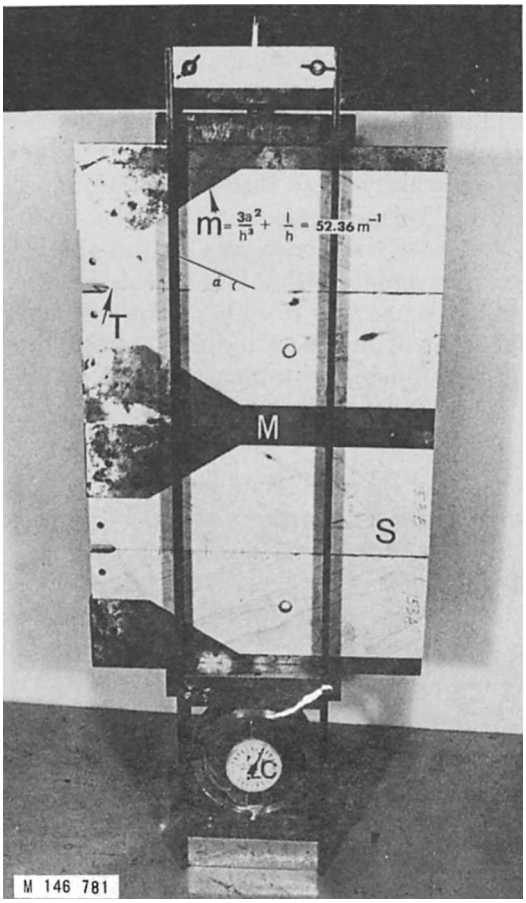

Fig. 1. Press for specimen preparation, capable of holding two specimens simultaneously.

tigated further by storing a quantity of the resin in an open can under a working fume cupboard. A slow rise in viscosity due to the alcohol evaporation was noted. PRF resins are deficient in formaldehyde and do not increase in viscosity when stored at room temperature. For a period of 2 weeks, samples were taken intermittently from the resin and then mixed with 10 parts per hundred (phr) resin, walnut shell flour, and 10 phr paraformaldehyde. The initial viscosity of the adhesive was determined with a Brookfield viscometer. Bonding was carried out as described above. The adhesive formulation was 100/10/10 (i.e., resin/paraformaldehyde/filler, weight basis).

Microscopy

Scanning Electron Microscopy

Scanning electron microscopy was used to observe the fine details of the fracture morphology. A Hitachi Model HUS-4GB evaporator was used for chromium-shadowing the specimens (10 × 5 × 2 mm) at a pressure of <

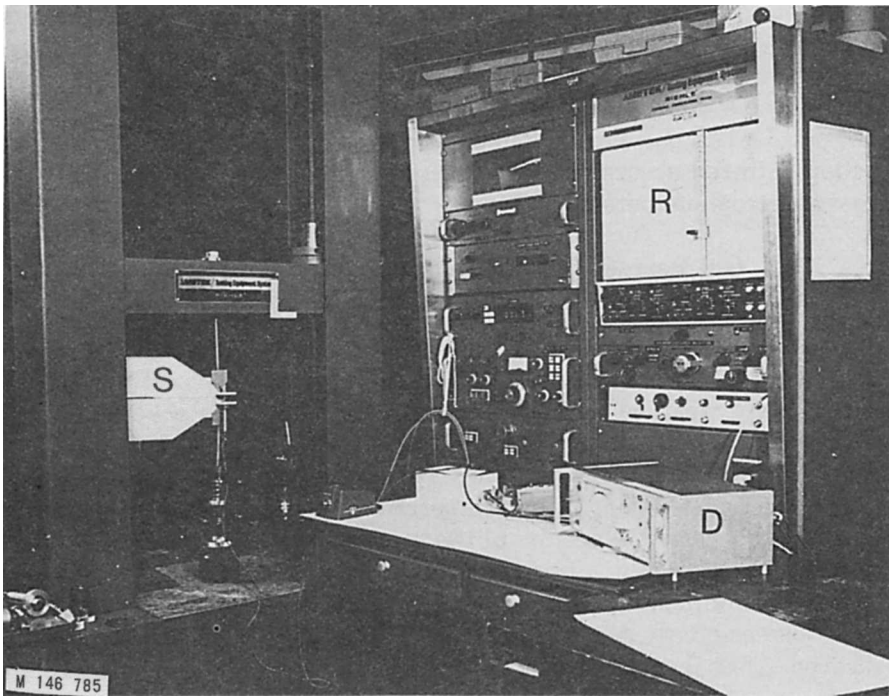

Fig. 2. Cleavage fracture testing of specimen(s) on test machine (Riehle Ametek) with Daytronic Signal Conditioner (D) and Hewlett-Packard X-Y Recorder (R).

10^{-5} mm Hg. Scanning electron micrographs of the specimens were taken using a Cwickscan 100 Model field emission microscope. In some cases, the micrographs were taken using a Cambridge Scientific Instrument Stereocam scanning electron microscope type 96113 Mark 2A. In these cases, a Denton Vacuum Desk-1 Cold Sputter-Etch Unit was used for gold-shadowing the specimens at a pressure of 7.0×10^{-3} mm Hg.

Fluorescence Microscopy

To determine the locus and type of failure, the fractured surface was examined by fluorescence microscopy utilizing ultraviolet (UV) radiation. In addition, serial sections (cross section and tangential oblique section) of the wood were examined to trace the depth and distribution of adhesive in the wood cells. The optical microscope employed was a Leitz Ortholux with mercury lamp [having a UG-1 (Leitz) filter and peak transmission at 365 μm] as the source. The natural bluish autofluorescence of the wood readily contrasted with the dark-red/brown mass of the adhesive facilitating the identification of the location of the adhesive. The photomicrographs were taken with a 35 mm Kodak Plus-X Pan film (PX-135).

Infrared Spectroscopic (IR) Studies

During bonding, a portion of each adhesive formulation (usually 30 g) was transferred to a metal can and then cured under the same conditions (in the same oven for the same cure time) as the adhesive joint. Soon after

removal from the oven, the adhesive was placed in a thick, tightly sealed (ziplock) polyethylene bag and stored in a sub-0°C room until IR measurements were made. For the infrared measurements, a small portion of the cured adhesive was ground to a fine powder, mixed with potassium bromide (KBr) powder (1.5 parts resin/300 parts KBr, weight basis) and pressed into a pellet. Infrared absorption scans were carried out on a Beckman 12 infrared spectrophotometer.

Gel Permeation Chromatography (GPC) and Solubility Measurements

For these measurements, the remaining portion of the cured adhesive from the metal can was ground to 20 mesh. Ten grams of the ground adhesive were weighed into an extraction thimble. This was placed in a specimen bottle containing 100 mL of tetrahydrofuran (THF). This amount of THF was sufficient to completely cover the adhesive. The bottle was sealed tightly and left at room temperature (ca. 24°C) for 5–6 weeks. At the end of this period, a portion of the solution was filtered and 6–10 mils of the filtered solution was injected into the chromatograph (Walters Model 501) which contained five styreagel columns in series. THF was used as the mobile solvent phase. A range of molecular weights of $<10^4$–10^8 could be measured. After the GPC measurement, the thimble was then removed and dried in an oven at 70–72°C to a constant weight. A chromatogram of the uncured resin was also obtained by injecting a 1% THF solution of the resin into the chromatograph.

RESULTS AND DISCUSSION

Differential Scanning Calorimetry

Figure 3 typifies the general thermal behavior of all formulations studied irrespective of the filler used in the particular formulation. For the pure resin, an endothermic peak appeared at about 195°C [Fig. 3(A)]. The endotherm persisted even with the addition of either paraformaldehyde or filler or both as seen in thermograms B, C, and D of Figure 3. However, the position of the endothermic peak generally shifted to lower temperatures with increasing amount of paraformaldehyde (thermogram D in Fig. 3). The heat of reaction at the endotherm, ΔH_{endo}, generally increased with increasing amount of paraformaldehyde as shown in Figure 4. At any given paraformaldehyde concentration, ΔH_{endo} did not change conspicuously with a change in the amount or type of filler. ΔH_{endo} at two levels of filler, 100/10/10 and 100/10/20, (resin/paraformaldehyde/filler phr, weight basis) was found to be the same for all the fillers. Chow, using differential thermal analysis (DTA), has also observed that phenol–resorcinol–formaldehyde (PRF) resins without added paraformaldehyde exhibit only an endothermic peak.[9] He attributed the endotherm to removal of water and other chemical reactions in the resin. The position of the endotherm in Chow's studies (100–120°C) differs from that in ours (ca. 180–210°C). However, we have to point out that Chow used DTA which obviously employed unsealed pans

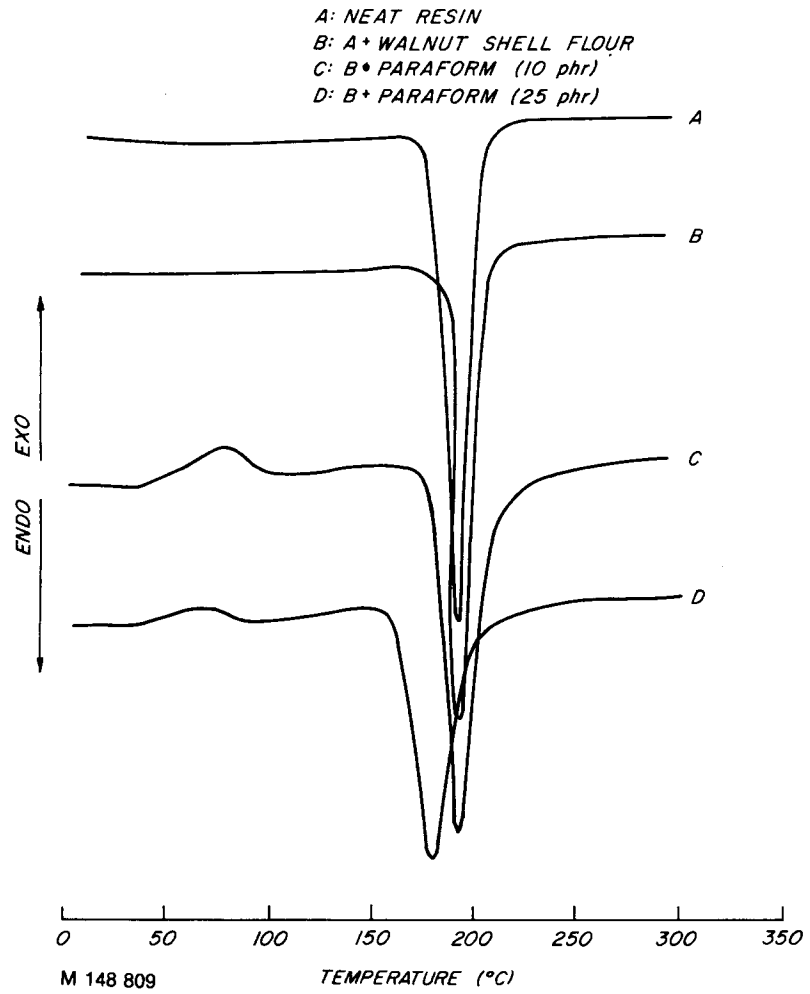

Fig. 3. Representative DSC thermograms for the adhesive formulations. Observe that thermograms A and B (formulations without paraformaldehyde) exhibit only endotherms. Notice, however, that thermograms C and D (formulations with added paraformaldehyde) show an exotherm in addition to the endotherm. Positions of both the exotherm and endotherm shift to lower temperatures with increasing paraformaldehyde concentration. (A) Neat resin; (B) A + walnut shell flour; (C) B + 10 phr paraform; (D) B + 25 phr paraform.

(in contrast to the sealed pans used in our studies). He used a heating rate of 6°C/min vs. 10°C/min in our studies, and the paraformaldehyde concentration used, which can influence the position of the endotherm, was not specified.

With the addition of paraformaldehyde, an exothermic peak appeared in the thermogram. (Compared thermograms C and D with A and B in Fig. 3.) Notice that the adhesive formulations containing only fillers and no paraformaldehyde did not show this exothermic peak. (Compare thermogram B with C and D in Fig. 3.) This type of behavior was observed irrespective of the type of filler used. The exothermic peak occurred at 95°C for a paraformaldehyde concentration of 5 phr. Further increase in the

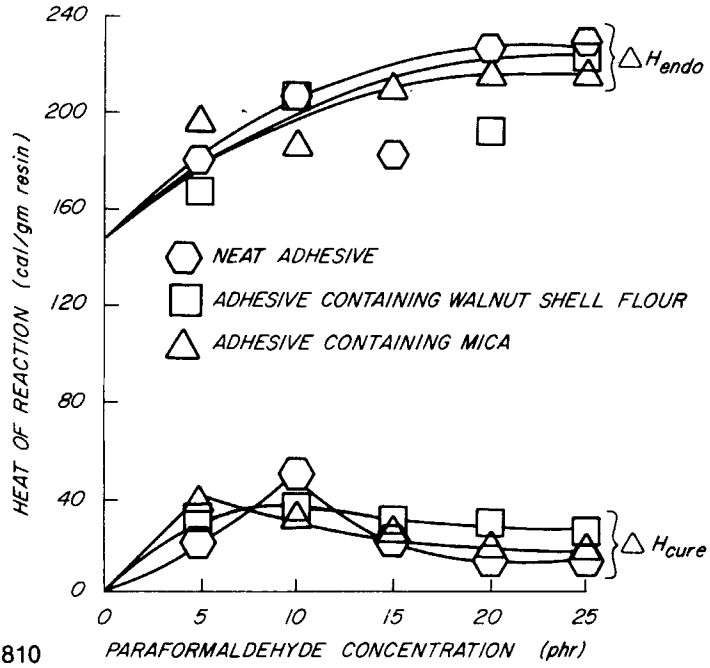

Fig. 4. Variation of heat of reaction with paraformaldehyde concentration. Observe that generally the heat evolved at the cure exotherm (ΔH_{exo}) and the heat absorbed at the endotherm (ΔH_{endo}) appeared independent of the type of fillers in the adhesive formulation; they depended only on the paraformaldehyde concentration: (△) neat adhesive; (□) adhesive containing walnut shell flour; (△) adhesive containing mica.

paraformaldehyde concentration resulted in a nearly linear decrease in the temperature of the exothermic peak as exemplified in Figure 3 (compare thermograms C and D) and seen graphically in Figure 5. The temperature at which the exothermic peak occurred depended only on the paraformaldehyde concentration and was independent of the type and/or concentration of the fillers. The heat of reaction at the exotherm, ΔH_{exo}, generally showed a maximum with increasing paraformaldehyde concentration. However, at any given paraformaldehyde concentration, the value of ΔH_{exo} was not conspicuously affected by the type or amount of filler. Our results are in agreement with those of Chow,[9] who also observed that the exothermic reaction occurred only in PRF adhesives containing paraformaldehyde. Incidentally, the exothermic peak in Chow's studies occurred at 85°C, which corresponds to the temperature of the exotherm of the adhesive formulation containing 10 phr paraformaldehyde in our studies.

From the above results two general conclusions are evident:

1. The thermal behavior of PRF resins shows two distinct regimes of activity: a low-temperature exothermic reaction which occurs only in adhesive formulations containing paraformaldehyde and a high-temperature endothermic reaction whose appearance is independent of the presence of either paraformaldehyde or filler or both.

2. The presence and nature of fillers used in this study have no significant effect on the cure characteristics of PRF resin.

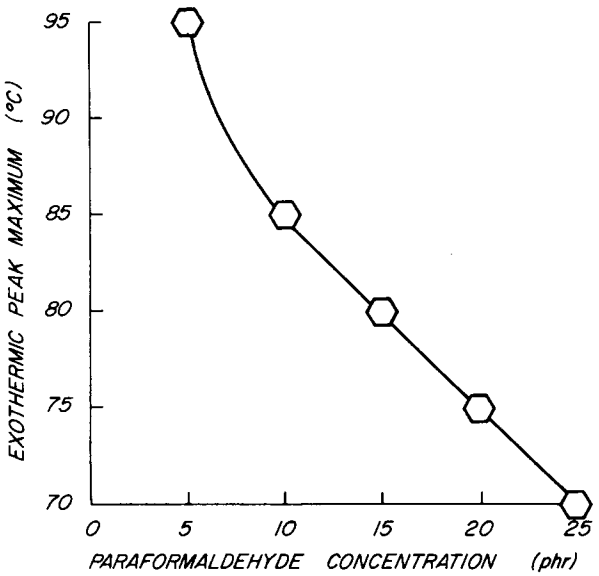

Fig. 5. Decrease of exothermic reaction temperature with increasing paraformaldehyde concentration.

Infrared Measurements

The infrared spectrum of the pure resin is shown in Figure 6, spectrum A. The absorption bands and their corresponding assignments are shown in Table II. A comparison of the spectrum of the adhesive formulation with 10 phr paraformaldehyde and no fillers, i.e., 100/10/0, with the spectrum of the pure resin, spectra C and A, respectively, in Figure 6, shows that the absorption bands marked with arrows in spectrum A (Fig. 6) and with an asterisk (*) in Table II disappeared completely. The absorption bands, 3400, 1610, 1517, and 1045 cm^{-1} decreased slightly while the bands 2925 and 1100 cm^{-1} increased slightly. The other absorption bands remained relatively unchanged.

Spectrum B (Fig. 6) typifies the spectra of adhesives cured without paraformaldehyde. Notice that the spectrum is essentially the same as that of the pure resin (spectrum A, Fig. 6). Observe in particular that the absorption bands which disappeared in the spectra for adhesives with added paraformaldehyde are still present in this spectrum.

The spectra of the adhesive formulation with and without filler, i.e. 100/10/10 and 100/10/0 are identical. Compare spectra A in Figures 7 and 8 with spectrum C in Figure 6. The only observable difference between these spectra is due to the absorption bands of the fillers themselves. Spectra A in Figures 7 and 8 are typical of the cured filled adhesives while spectra B in these figures represent the spectra of fillers alone.

Chow[9] has reported that PRF resins with resorcinol contents greater than 5% exhibit two strong bands: 960 and 1140 cm^{-1}. He attributed the presence of these bands to resorcinol noting that these bands were assigned by Nakanishi[15] to in-plane bending modes of hydrogen atoms in 1,3 substituted ring. In a subsequent paper, Chow and Steiner[12] used the 960 cm^{-1}

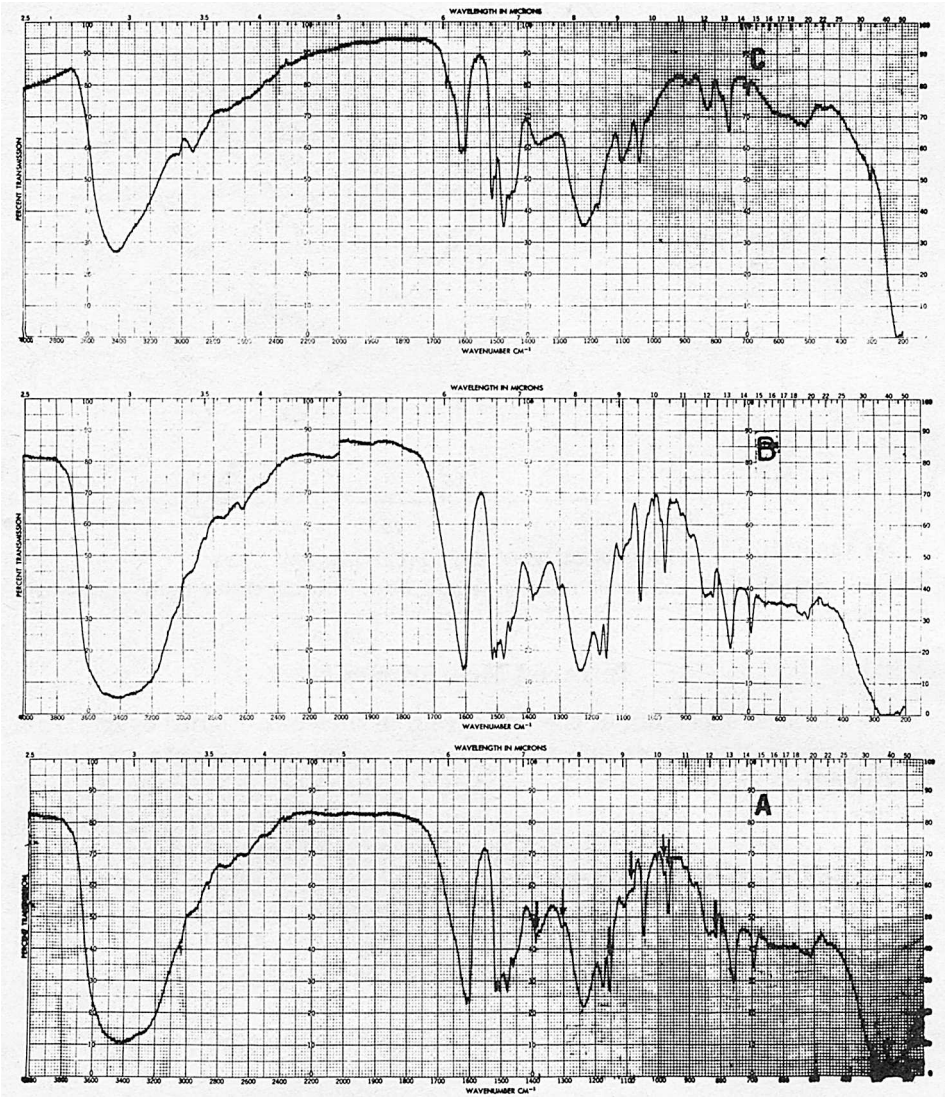

Fig. 6. Infrared absorption characteristics of resin: (A) parent (pure) resin; (B) parent resin cured at 85°C for 1 h; (C) parent resin plus 10 phr paraformaldehyde cured at 85°C for 1 h. Notice that there is essentially no difference between A and B, but observe that the bands marked with arrow in A have disappeared in C.

band to determine the resorcinol content of commercial and laboratory-synthesized PRF resins. Chow[9] had further observed that, without addition of paraformaldehyde, the 960 cm^{-1} band maintained a relatively constant intensity even when heated to 145°C. However, with added paraformaldehyde, the 960 cm^{-1} band disappeared at a temperature of about 80°C. Our results are in complete agreement with this observation.

The observed decrease in the 1045 cm^{-1} band assigned to the methylol group and the increase in the 1105 cm^{-1} band assigned to the dimethylene ether linkage are consistent with the work done by Yamao et al.[13] These authors studied both acid hardening and heat curing of resole type phenolic resins using infrared spectroscopy. They reported that methylene ether

TABLE II
Infrared Absorption Bands of Phenolic Resins

Wave number (cm^{-1})	Assignment[a]	Comments
3400	ν_{OH}	Polymeric OH give broad band
3030	ν_{CH}	=C—H stretching vibration (masked by broad =H band)
2925	ν_{CH}	In-phase stretching vibration of —CH_2— hydrogen atoms
2850	ν_{CH}	Out-of-phase stretching vibration of —CH_2— hydrogen atoms
1610	$\nu_{C=C}$	Characteristic skeletal stretching mode of the semi-saturated carbon-carbon bonds of benzene ring
1600		
1517		
1504		
1480	$\nu_{C=C}$	Strong sharp band characteristic of 1, 2, 3, 5 and 1, 2, 3 substituted benzene due to semiunsaturated C—C bands of benzene ring
1460	δ_{CH}	—CH_2— deformation vibration
1450	$\nu_{C=C}$	Benzene ring C—C skeletal stretching vibration; obscured by —CH_2— deformation band
1390*	δ_{OH}	OH deformation vibration in polymeric phenol
1378	δ_{C-CH_3}	C—H symmetric deformation vibration of aliphatic hydrocarbon groups
1305	δ_{OH}	OH deformation vibration of primary alcohol
1237		In-plane bending vibration of phenolic OH (broad)
1175*		In-plane bending vibration of aromatic CH
1153*		In-plane bending of hydrogen atoms in 1,3 substituted aromatic ring
1100	ν_{C-O-C}	Antisymmetric stretching vibration of —CH_2—O—CH_2—
1075*		In-plane bending vibration of aromatic CH
1045	ν_{C-O}	Single bond C—O stretching vibrations of ethers and in structures containing —CH_2OH group
1000		Aliphatic hydroxyl
976*		1, 2-, 1, 2, 3-, and 1, 2, 4-Benzene ring substitution
965*		In-plane bending mode of hydrogen atom in 1,3 substituted aromatic ring
910		Methylene bridge
885	δ_{CH}(out of plane aro-	Isolated H
835	matic)	
814*		Adjacent 2H
780		
760		Adjacent 3H and 4H
694		Adjacent 5H

[a] We do have to emphasize that the literature assigned absorption bands to the various chemical groups did vary, as might have been expected. For example dimethylene ether ν_{C-OC} has been variously assigned 1100 cm^{-1}, [10] 1064 cm^{-1}, [11], 1050 cm^{-1} while the methylol OH group ν_{C-O} had been assigned 1045 cm^{-1}, [10] 1040 cm^{-1}, [9] 1010 cm^{-1}, [12,13] 1000 cm^{-1}, [11] 1050 cm^{-1}, [14] 1058 cm^{-1}.[21]

bond formation, due to reactions between methylol groups, is the initial major reaction. The ether linkages subsequently decomposed into three possible products [eqs. (4)–(6)]. The extent and rate of this decomposition depended on the formaldehyde/phenol (F/P) mole ratio and the reaction temperature.

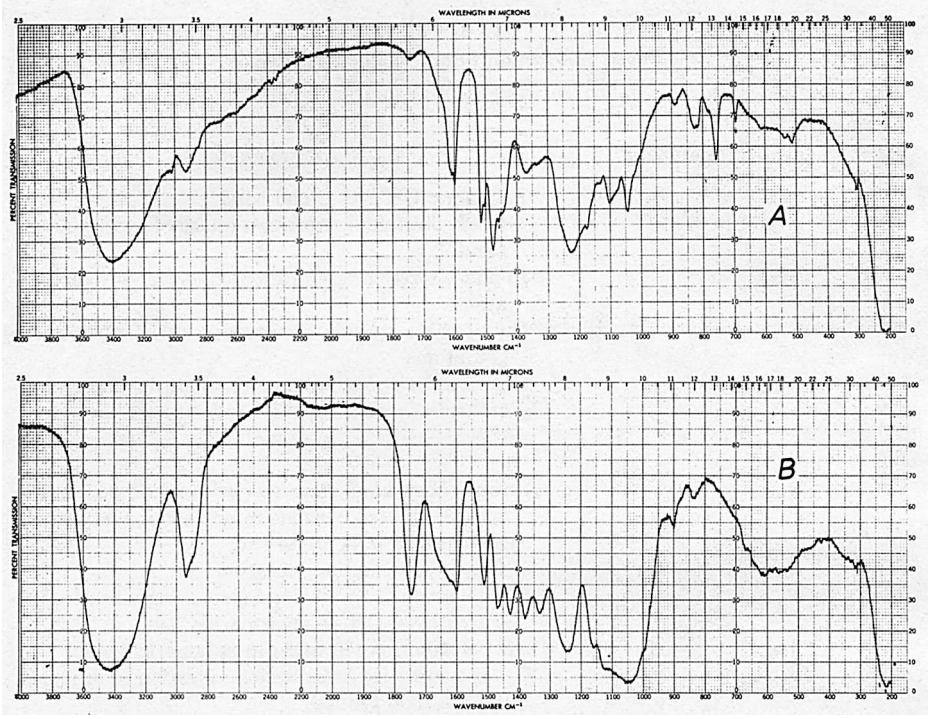

Fig. 7. Infrared absorption of adhesive filled with walnut shell flour (A) compared with that of the filler alone (B). Adhesive formulation: 100/10/10; cured at 85°C for 1 h. Note the similarity between spectra A in Figures 7 and 6.

We concluded from the results of DSC measurements that of the two regimes of thermal activity exhibited by PRF resin, the low temperature reaction exotherm was due to added paraformaldehyde. Results from infrared studies of these resins not only substantiate this conclusion, but also provide evidence indicating that the exotherm is due primarily to resorcinol–formaldehyde reactions.

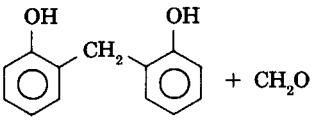

(4)

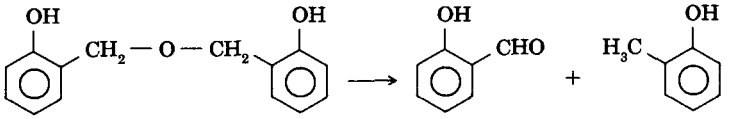

(5)

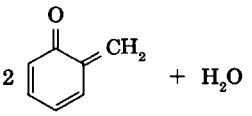

(6)

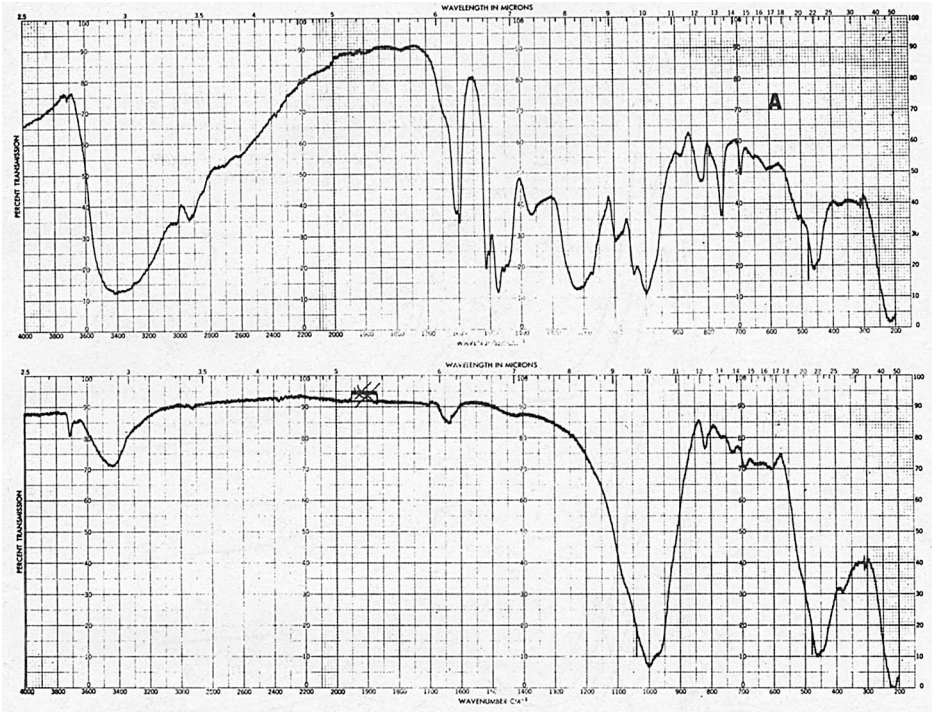

Fig. 8. Infrared absorption characteristics of adhesive filled with mica (A) compared with that of mica alone (B). Adhesive formulation: 100/10/10; cured at 85°C for 1 h. Also note the similarity between spectra A in Figures 8 and 6.

Gel Permeation Chromatography and Solubility Measurements

Figure 9 shows the gel permeation chromatograms of the soluble fractions of the adhesive formulation (100/10/10) containing various fillers (B–G) relative to those of the neat adhesive (adhesive without filler, A) and the parent resin (----). The adhesives were derived from the commerical resin (G4411) and were cured for 1 h at 85°C. Three distinct peaks, I, II and III (i.e., three separate molecular weight species), are evident in both the soluble fraction of the adhesive and the parent resin. Notice, however, that peaks for the species in the adhesives occuring at 183, 189, and 201 mL, respectively, are displaced to lower retention volumes relative to corresponding peaks in the parent resin, i.e., 184, 197, 205 mL, respectively. It thus appears that the size (molecular weight) of each soluble species in the adhesives has increased relative to that of the corresponding species in the parent resin. In the parent resin, the relative order of abundance or amount of the species is II > III >> I. But in the soluble fraction of the adhesives the relative order of abundance of the species is III > II > I. Apparently during the cure process, species II is consumed at a faster rate than species III. Notice in particular that the retention volumes and the relative amount of the three species are, within the limits of experimental error, quite similar for all the adhesives irrespective of the filler used. It is also noteworthy that the soluble fractions of the cured adhesives (both filled and unfilled) were about 36% in all cases. This lends further support to our previous conclusion

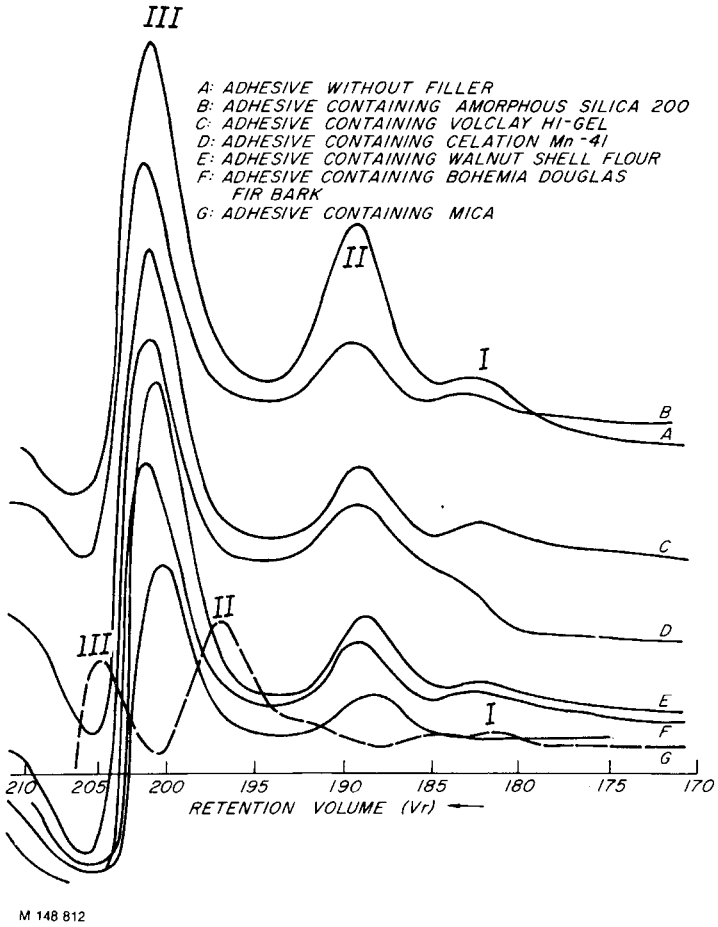

Fig. 9. Gel permeation chromatograms of adhesive 100/10/10 filled with various fillers (A–G) relative to that of the parent resin (---). Note that three distinct species I, II, and III are present in both the soluble fraction of the adhesives and the parent resin. Observe in particular that the chromatograms for the various adhesives are not considerably different: (A) without filler; (B) containing amorphous silica 200; (C) containing Volclay Hi-Gel; (D) containing Celation Mn-41; (E) containing walnut shell flour; (F) containing Bohemia Douglas fir bark; (G) containing mica.

from DSC and infrared absorption results that the type or nature of filler used in these studies do not have a noticeable effect on the cure characteristics of PRF resins.

Fracture Tests

Effect of Filler Type

Table III illustrates the effect of the change of filler type on the fracture energy of the resulting adhesive joint. It is obvious from the table that, with the adhesive formulation (100/10/10) and cure conditions (85°C cure for 1 h) used in these tests, filled adhesives did not always yield joints with better strength performance than the unfilled adhesive. The degree of

TABLE III
Effect of Filler Type on Joint Fracture Energy

Adhesive formulation			Fracture energy (J/m²)			Brittleness index I ($\Delta G_I/G_{Ic}$)
Resin[a]	Paraform	Filler	G_{Ic}	G_{Ia}	ΔG_I	
Unfilled adhesive						
100	10	0	43.00	31.19	11.81	0.27
A. Lignocellulosic (organic)						
Walnut shell flour						
100	10	10	64.24	48.75	15.49	0.24
Bohemia Douglas fir bark						
100	10	10	27.78	22.47	5.31	0.19
B. Inorganic						
Mica						
100	10	10	39.99	34.69	5.30	0.13
Volclay-Hi Gel						
100	10	10	29.37	25.58	3.79	0.13
Celaton MN 41						
100	10	10	26.04	22.98	3.06	0.12
Amorphous silica 200						
100	10	10	49.75	26.89	22.86	0.46

[a] The resin used was Koppers Penacolite G4411.

strength improvement was minimal in the case of some filled adhesives. From the organic group of fillers, walnut shell flour had the greater joint-strengthening characteristics while amorphous silica 200 exhibited the highest joint-strengthening qualities within the inorganic fillers. Between both groups of fillers, however, walnut shell flour resulted in joints with the highest energy.

The fracture characteristics of the joints further divided the joints into two distinct groups.

Group I: those that failed by unstable crack propagation, viz., joints from the unfilled adhesive, adhesives filled with organic fillers and amorphous silica 200.

Group II: those that failed by stable crack propagation, viz., joints from adhesives filled with the inorganic fillers. Typical actual load–deflection data representative of these modes of failure are shown in Figure 10. Furthermore, both visual and SEM examination of the fracture surfaces revealed that, for joints that failed by unstable crack propagation (group I), the crack went back and forth between the faces of the two adherends. That is, in this case, the locus of failure was a combination of interfacial and cohesive modes within the adhesives. Typical SEM micrographs of the fractured surfaces are shown in Figures 11 and 12. On the other hand, for joints that failed in a stable manner (group II), failure was completely cohesive within the adhesive. In addition, the fractured surfaces of this group were composed virtually of filler particles. [Compare the SEM micrograph typical of these fractured surfaces with that of the corresponding filler (Fig. 13).] Observe that the only conspicuous difference between micrographs A and B is the relative amount and compactness of fillers. The filler particle morphology in micrograph A (fractured surface) is very similar to that of the pure fillers in micrograph B, indicating relatively little adhesion of the resin to the filler particles.

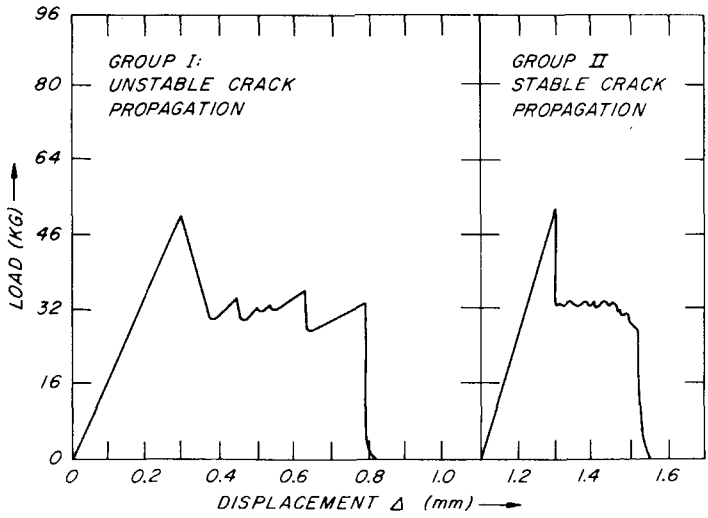

Fig. 10. Differences in adhesive chemistry as reflected by failure characteristics. Group I: joints from unfilled adhesive, and those filled with walnut shell flour, Bohemia Douglas fir bark and amorphous silica 200: Group II: joints from adhesives filled with mica, Volclay Hi-Gel, and Celaton MN 41. Adhesive formulation: 100/10/10 cured for 1 h at 85°C.

On a given test machine and at a given crosshead speed, the difference between initiation and arrest fracture energies, $G_{I_c}-G_{I_a}$, is a measure of the brittleness or resistance to catastrophic failure of the adhesive system. Generally, this difference increases with increasing G_{I_c}, i.e., the stronger the adhesive system the more susceptible to catastrophic brittle failure it becomes. Here we introduce a brittleness index I defined as

$$I = \frac{G_{I_c}-G_{I_a}}{G_{I_c}} \tag{7}$$

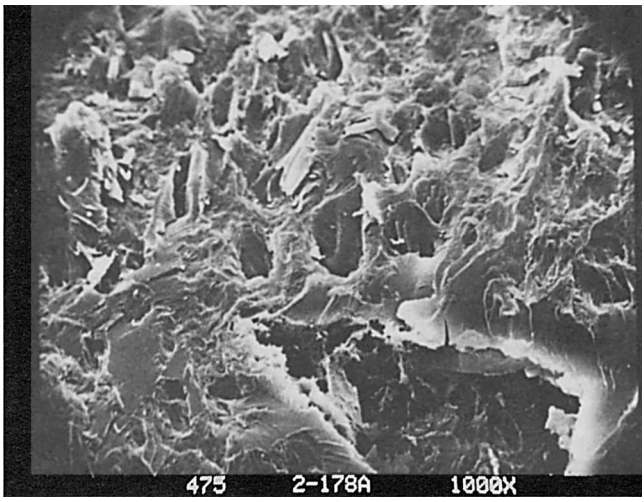

Fig. 11. Scanning electron micrograph of the fractured surface of specimen derived from unfilled adhesive.

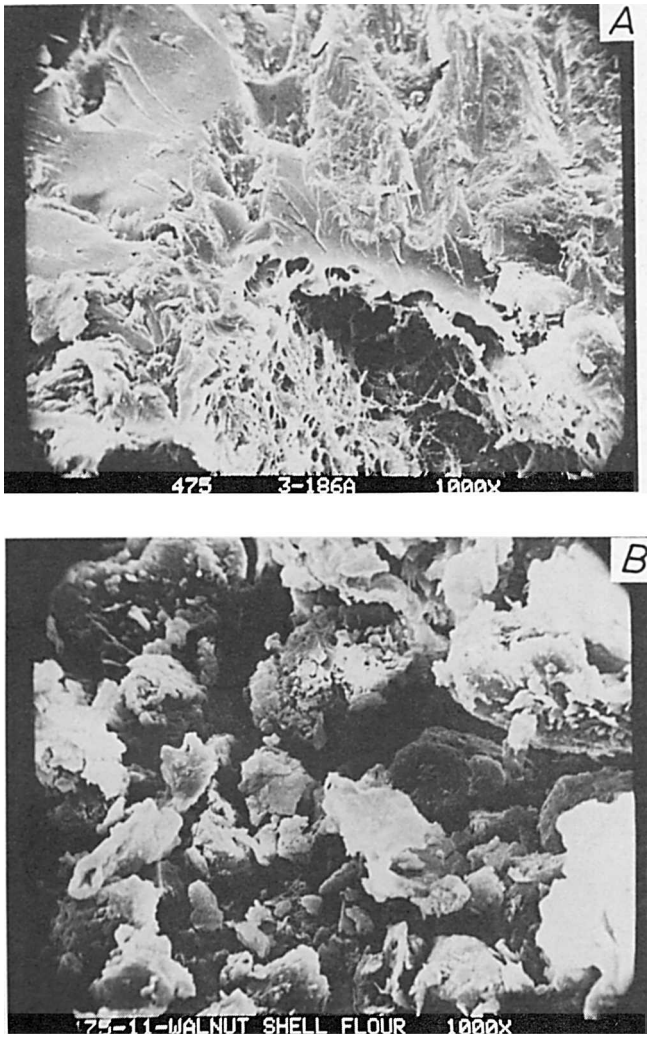

Fig. 12. Scanning electron micrograph of the fractured surface of a joint derived from adhesive filled with walnut shell flour (A). Micrograph is typical of Group I type joints. Scanning electron micrograph of filler walnut shell flour (B). Note the similarity between A and Figure 11. Observe that the structural features of the filler are not identifiable in A.

That is, the brittleness index I is a normalization of the energy released during failure with respect to the energy stored in the system just at the onset of crack propagation. For an ideally brittle system, the first crack is the last and only crack; i.e., $G_{I_a} = 0$. Consequently, $I = 1$. For a system which is capable of extensive plastic deformation, once the crack is initiated it is quickly blunted. The same is true for systems which are weak and discontinuous. For these systems $G_{I_c} \approx G_{I_a}$ so that $I = 0$. It must be mentioned that $G_{I_c} - G_{I_a}$ can be rate-sensitive and sensitive to the inertial effects of the testing machine. Hence, all specimens were tested in the same manner, using the same fixtures and jaw separation rates.

The brittleness index I for the joints from the various adhesive formulations is tabulated on the last column of Table III. Notice that, apart from

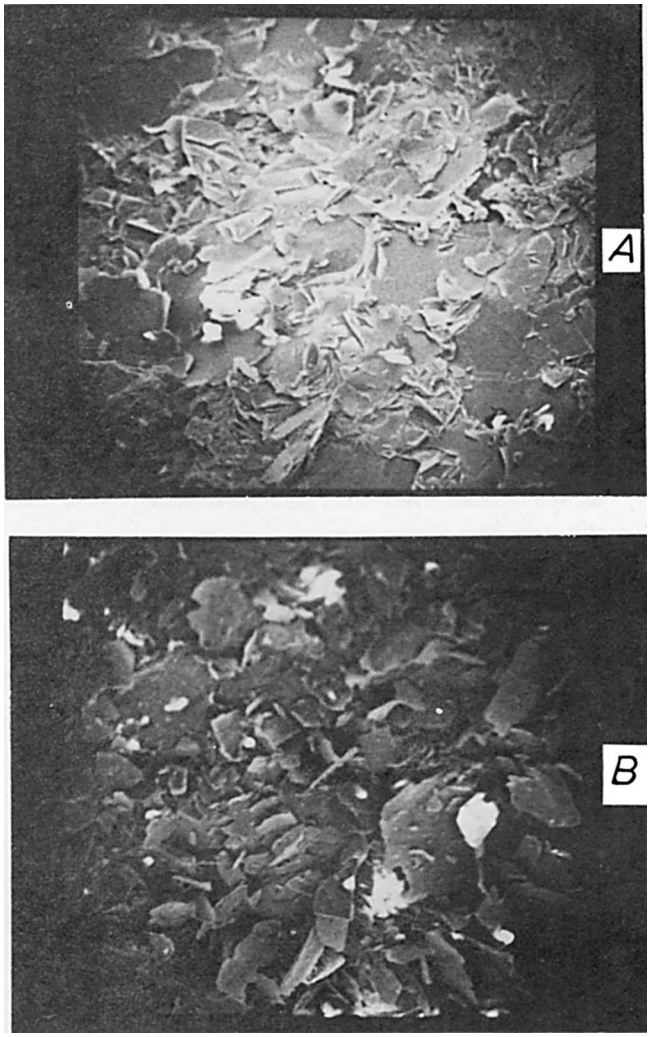

Fig. 13. Scanning electron micrographs of the fractured surface of adhesive filled with mica (A) [typical of group II type joints] and that of mica alone (B). Observe the similarity between the two micrographs.

the joint derived from the adhesive filled with amorphous silica 200, the joint from the unfilled adhesive was more brittle than those from filled adhesives. In general, joints from adhesives filled with the organic fillers were more brittle than those derived from adhesives containing inorganic fillers.

It is perhaps necessary to recap the peculiar or "anomalous" characteristics of joints derived from the adhesive filled[2] with amorphous silica 200:

1. The fracture energies of these silica filled joints were much higher than those of joints derived from adhesive filled with other inorganic fillers.
2. The fracture characteristics were indicative of unstable crack propagation in contrast to the stable crack propagation exhibited by the other inorganic filler containing adhesives.
3. The joints from this adhesive were very brittle, even more brittle than the unfilled adhesive.

A number of authors have also studied the effect of fillers on adhesive joint performance. Vick,[16] using shear block lumber-to-lumber joints and three adhesive formulations, each of which contained either asbestos, walnut shell flour, or wood flour fillers, reported that the values of dry shear strength and wood failure for the three filled adhesives were not as high as joints made with unfilled PRF adhesives. This difference in the strength of joints from filled and unfilled adhesives was found only in the case of thick gluelines. Rice[17] investigated the effect of urea–formaldehyde (UF) resin viscosity on plywood bond durability. Examination of his data reveals that, for adhesive joints derived from adhesives of the *same low viscosity* (thin gluelines), joints from filled adhesives (filler used was pecan wood flour) had higher shear strength and percent wood failure than joints from unfilled adhesives. However, when the adhesive viscosity was high (thick gluelines), joints from filled adhesives had poorer strength values than those from unfilled adhesives. Using a viscosity range of 3400–6000 cp, Strickler and Sawyer[18] investigated the possibility of replacing furafil (derived from corn cobs) with attapulgite clay (an acicular hydrous magnesium aluminum silicate) as filler in exterior plywood adhesives. Their test results demonstrated that adhesive formulations containing attapulgite clay substitutions of 50 and 100% for furafil did not decrease bond strength. Quirk et al.[19] have obtained results which showed that bonded butt joints decreased in strength with increasing adhesive viscosity.

While our DSC, IR, GPC, and solubility studies have consistently reinforced the argument that fillers did not significantly affect the cure characteristics of an adhesive, our fracture tests and the other studies in literature show that the performance of an adhesive joint is a strong function of the presence and nature of the filler used in the particular adhesive formulation. The work of the authors cited above does show that the type of effect fillers had on adhesive joint performance depends primarily on the viscosity of the adhesive formulation. We do not have sufficient information on the physical and chemical characteristics of the fillers used in both our experiments and the other studies to be able to give an all-embracing rationalization of the various results. However, from the scanning electron micrographs of the fractured surfaces, it is evident that the weak link and, hence, the locus of failure in an adhesive joint is greatly determined by the extent of interaction between the adhesive and the fillers. In general, where the interaction between the adhesive and the fillers was significant, high fracture energies were obtained. On the other hand, joints derived from adhesives, where the interaction between the adhesives and fillers was small, failed essentially by a tearing apart of the continuous weak link between the filler particles.

Effect of Initial Resin Viscosity

From the brief literature review in the last section, it is obvious that the effect of fillers on joint performance is contingent on the base resin viscosity. To pursue this subject further, we changed the initial viscosity of the adhesive as described earlier. In addition, we probed the locus of failure and resin distribution by fluorescence microscopy of both the fractured surfaces and serial sections of the adherends.

Figure 14 shows the effect of initial resin viscosity on fracture energy. Observe that the fracture energy first increased with the viscosity of the resin and then dropped rather sharply to a somewhat constant value with further increase in resin viscosity. Micrographs from fluorescence microscopy were carefully scrutinized. The following general observations, typified by the photomicrographs in Figures 15–19 (which were selected to be as truly representative of the overall trend of behavior), can be made:

1. The less viscous the resin the greater the extent of penetration into the porous structure of the wood. (Compare Figs. 15 and 16.) Figure 15 is a serial section of an adherend from joints derived from a resin viscosity of 729 cp while Figure 16 is that of adherends from joints obtained from a resin of viscosity 3500 cp.

2. Extensive penetration of the fiber walls was not evident. Figure 17 shows typical serial sections down through the wood surface.

3. Failure of the joints was largely interfacial, with the crack passing back and forth between the faces of the two adherends. Most of the adhesive remained on the fractured surfaces of the adherend with greater adhesive penetration, indicating that, during crack growth, the crack remained in close proximity of the adherend surface little penetrated by the adhesive. (Compare micrographs A and B in Figs. 15–17.) Observe that in all cases the layer of adhesive on the fractured surface, micrograph A, is thicker than that on the opposite surface, micrograph B. In addition, note that the extent of adhesive penetration is greater in A than in B. It, therefore, follows that the weak link in the adhesive joint is related to the extent of adhesive penetration into the porous adherends. However, there is not necessarily a direct correlation between fracture energy and the depth of adhesive penetration. The adherends with the greatest adhesive penetration did not produce the joint with the highest fracture energy.

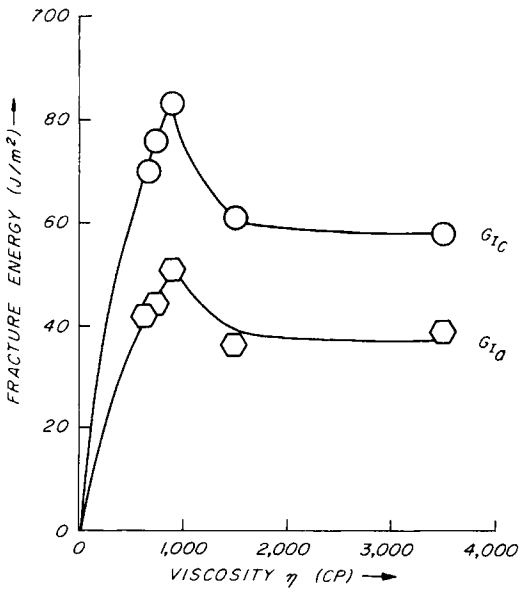

Fig. 14. Effect of initial resin viscosity on fracture energy.

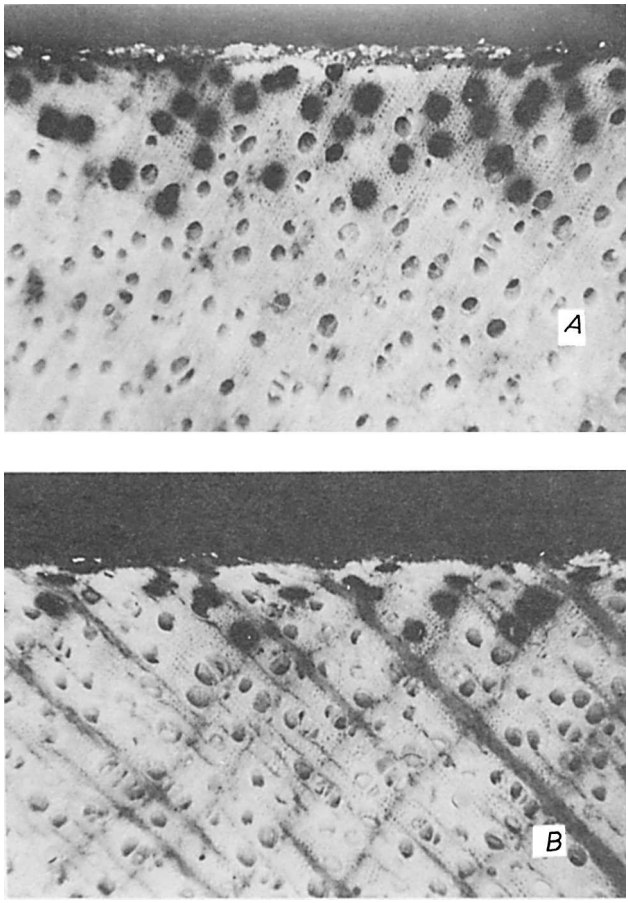

Fig. 15. Photomicrographs of cross section of adherends from the joint derived from resin of viscosity 660 cp: (A) photomicrograph of one adherend; (B) photomicrograaph of the side of the second adherend directly opposite to A. Note that the thickness of the adhesive layer and the depth of penetration are greater in A than B.

4. Photomicrographs of the fractured surface of the joint with the highest fracture energy in Figure 14 revealed a unique characteristic: wood failure (Fig. 18). The white circular areas in Figure 18 and micrograph A of Figure 19 represent filler particles (walnut shell flour) while the dark areas with distinct fibrous structure represent "adhesive-soaked" wood. Note in particular from these figures that adhesive-soaked fibrous wood structure (dark) generally terminates on the fracture surface as a whitish area. This white area, i.e., the root of the adhesive-soaked wood structure, represents the wood immediately surrounding the soaked wood. Apparently, after cure, the adhesive within the penetrated wood structure reinforces or strengthens these soaked structures. This imposes some stress in the wood in the immediate vicinity of the penetrated wood, i.e., each adhesive-soaked wood is surrounded by a zone of weakness. Crack growth seemed to have occurred by failure in adhesion to the filler particles at the wood–adhesive interface. However, in this process, the weakened "roots" of the adhesive-soaked wood structures which are close enough to this interface are pulled out. In pre-

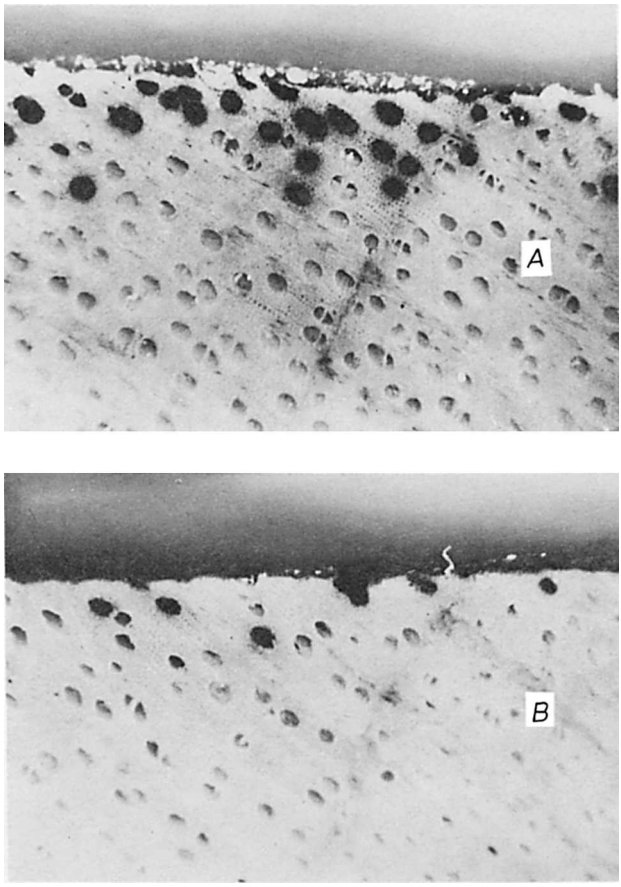

Fig. 16. Photomicrographs of cross section of adherends from joint derived from resin of viscosity 3500 cp. A and B are photomicrographs of the sections of the two adherends directly opposite each other. Note again that the thickness of the adhesive layer and the depth of penetration of adherend A are greater than in adherend B. Note also that the depth of penetration is less in this figure than in Figure 15 (viscosity 3500 cp vs. 660 cp).

vious publications,[1,7] we presented data which showed that where adhesive penetration was such that wood failure was induced, no matter how shallow, the resulting fracture energy was always high.

5. There appeared to be an abundance of fillers on the fractured surface of the adherends, particularly on the adherend surface with the thicker layer of adhesive (Figs. 18 and 19). This suggests that failure in adhesion to the filler particles and confirms that fillers play a vital role in determining the locus of failure.

From the preceding observations, it is evident that the rheological characteristics of an adhesive (reflected by the adhesive viscosity) fundamentally influence fracture energy. Addition of fillers to an adhesive considerably modifies its rheological behavior. The formation of a good joint depends largely on the degree of interaction between the adhesive and the adherends. A good joint, of course, is characterized by a continuous film of solid adhesive between the adherends and a penetration of the adhesive into the capillary structure of the wood to give sufficient anchorage. Extremes of viscosity

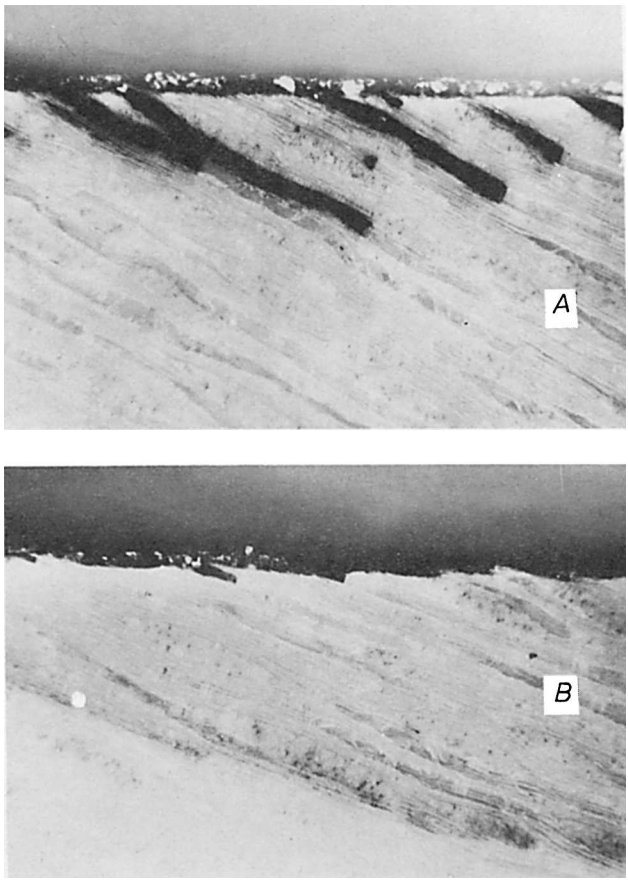

Fig. 17. Photomicrographs of tangential sections of directly opposing sides of two adherends from the same joint showing that during crack propagation; the crack remained in the close proximity of the adherend less penetrated by the adhesive (B).

Fig. 18. Photomicrograph of the fractured surface from joints with the highest fracture energy. Observe wood failure. White circular areas represent fillers (walnut shell flour). Note distinct fibrous structure (wood) soaked in adhesive (dark). Each fibrous structure terminates on the fractured surface with whitish area and indicates that the locus of failure occurred in the wood immediately surrounding the adhesive-soaked wood.

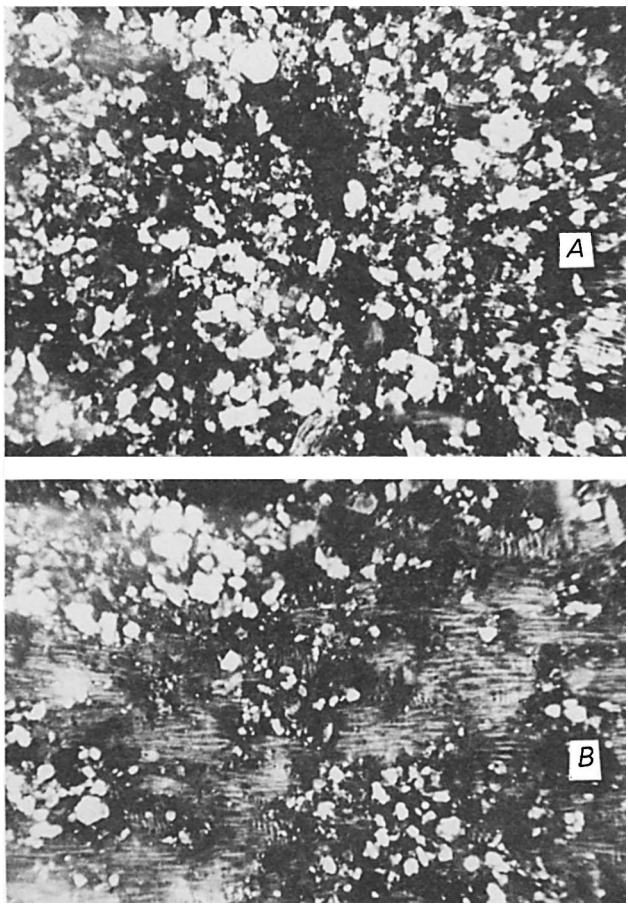

Fig. 19. Relative abundance of fillers (white areas) on the fractured surfaces of the opposing sides of the two adherends in a joint. Crack growth appears to have occurred by failure in adhesion between fillers and the adhesive.

are deleterious to the formation of strong and durable joints. A starved joint is obtained from adhesives of low viscosities which are quickly assembled and pressured. On the other hand, when adhesives with high viscosities are allowed to stand for a considerable time after spreading before pressure is applied, poor contact and penetration occur.[20] Klein[22] has stated that the desired goal is for the adhesive to penetrate at least four cells deep on each side of the glueline and completely wet the cell walls and other capillary surfaces. An "appropriate viscosity level" is, therefore, required for optimum joint performance. However, it is pertinent to ask what constitutes an appropriate viscosity level. This is determined exclusively by the chemical and physical characteristics of the adherends. These include the moisture content and the structure of wood (early wood vs. late wood, heartwood vs. sapwood, etc.) and the physical characteristics associated with wood processing.

The next logical question is: Given two adhesive formulations of the same viscosity and granted that the adherends for the two adhesive formulations

have the same characteristics, will strength of the resulting joints be the same? The answer to this question is: The joints will not necessarily have the same strength. The viscosity level of an adhesive ensures that the first and probably the most important prerequisites for good bonding are satisfied, viz., controlled wetting and penetration of the adherends (i.e., adequate interaction between the adherends and the adhesive). Stated differently, one might say that an appropriate viscosity level is a necessary but not a sufficient condition for maximization of joint strength. The chemical and physical properties of the adhesive components control the fracture path.

This brings us to the role of fillers in an adhesive. Apart from economic considerations, the primary role of fillers is in the development of the right viscosity level of the adhesive. Because of the difference in moduli between the fillers and the bulk adhesive, fillers alter the stress distribution in an adhesive joint under stress. Local stresses around the fillers appear to be of such magnitude as to induce fiber–fiber and/or wood–adhesive delamination or adhesive–filler separation. A controlled size and amount of such discontinuities can significantly increase strength properties. This is akin to the strengthening which occurs in filled thermoplastics where fillers are known to induce crazing and, hence, raise the strength of the homogeneous plastics. In the case of filled adhesives, however, the filler-induced discontinuities, if of the right kind and amount, render the Cook–Gordon crack-stopping mechanism[22] operative. The difference in the performance between two joints derived from two differently filled adhesives, therefore, depends on the size and amount of filler-induced discontinuities. In those cases where a measure of interaction exists between the fillers and the adhesive, the induced discontinuities act as crack stoppers or arrestors. On the other hand, where the interaction between the filler and adhesive is poor, the induced discontinuities readily form a continuous weak link in the joint. This reduces the possibility of achieving the maximum attainable joint strength. By the same token, in those cases where the interaction between the fillers and the adhesive is extremely high, the type of discontinuities described above will not be induced—i.e., in essence the filled adhesive behaves like the unfilled adhesive.

CONCLUSIONS

1. The fillers used, both organic and inorganic, did not affect adhesive cure.

2. The phenol–resorcinol–formaldehyde resin showed two distinct realms of thermal activity during cure: a low-temperature exotherm and a high-temperature endotherm.

3. The low-temperature exotherm is associated with the reaction between resorcinol and paraformaldehyde.

4. Inorganic fillers in general resulted in bonds which failed by stable crack propagation while organic fillers resulted in bonds which failed by unstable crack propagation.

5. Walnut shell flour produced bonds with the highest fracture energy and intermediate brittleness. Amorphous Silica 200 produced bonds of high

fracture energy and high brittleness. Douglas fir bark filler and the remaining inorganic fillers produced bonds with lower fracture energy and low brittleness. Unfilled adhesive bonds were intermediate in fracture energy and brittleness.

6. The effects of filler appear related to the physical aspects of adhesive viscosity, penetration into the wood, concentration of the filler in the bondline, shape of the particles, and the bond between the adhesive and the filler particle.

We wish to thank the Forest Products Laboratory, Madison, WI, and the Weyerhaeuser Corp. sincerely for the funding of this work. We are indebted to Dr. Roland Kreibich for the phenolic resin recipe and discussions about the results. We also wish to thank Dr. Robert Gillespie, Dr. George Myers, and Dr. Alfred Christiansen for their support, review, and critique of this work.

References

1. R. O. Ebewele, B. H. River, and J. A. Koutsky, *Wood Fiber.*, **11**(3), 197 (1979).
2. S. Mostrovoy, P. B. Crosley, and E. J. Ripling, *Mater.*, **2**(3), 661 (1967).
3. S. Mostovoy and E. J. Ripling, *J. Appl. Polym. Sci.*, **15**, 641 (1971).
4. E. J. Ripling, S. Mostovoy, and R. L. Patrick, *Adhesion*, STP 360; Am. Soc. for Mater. and Testing, Philadelphia, 1963, p. 5.
5. E. J. Ripling, S. Mostovoy, and R. L. Patrick, *Mater. Res. Stand*, **64**(3), 129 (1964).
6. E. J. Ripling, H. T. Corten, and S. Mostrovoy, *J. Adhesion*, **3**, 107 (1971).
7. R. O. Ebewele, B. H. River, and J. A. Koutsky, *Wood Fiber*, **12**(1), 40 (1980).
8. J. E. Robertson and R. R. P. Robertson, *Forest Prod. J.*, **27**(1), 30 (1977).
9. S. Chow, *Holzforschung*, **31**(6), 200 (1977).
10. L. J. Belamy, *The Infrared Spectra of Complex Molecules*, 2nd ed., Wiley, New York, 1958.
11. P. J. Secrest, *J. Paint Technol.*, **37**(481), 187 (1965).
12. S. Chow and P. R. Steiner, *Holzforschung*, **32**(4), 120 (1978).
13. M. Yamao, S. Nukui, and S. Tanaka, *Hippon Kagakukai-shi*, **5**, 914 (1972).
14. O. D. Shreve, *Synthetic Organic Coating Resins, Organic Analysis, Vol. 3*, Wiley-Interscience, New York, 1956.
15. K. Nakanishi, *Infrared Absorption Spectroscopy*, Holden-Day, San Fransisco, 1962, p. 26.
16. C. B. Vick, *Forest Prod. J.*, **23**(11), 33 (1973).
17. J. F. Rice, *Forest Prod. J.*, **15**(3), 107 (1965).
18. M. D. Strickler and E. W. Sawyer, *Forest Prod. J.* **24**(11), 17 (1974).
19. J. T. Quirk, T. T. Kozlowski, and R. F. Blomquist, USDA Forest Service Research Note FPL-0178, Dec. 1967.
20. T. R. Truax and E. Gerry, "A Study of the Permeation of Glue into Wood," USDA Forest Service, Forest Products Laboratory project report, Project L-157-6, 1921.
21. W. M. Jackson and R. T. Conley, *J. Appl. Polym. Sci.*, **8**(5), 2163 (1964).
22. J. A. Klein, FPRS Separate No. AM-75-S-67.

Received June 17, 1985
Accepted September 4, 1985